FOLIA HISTOCHEMICA ET CYTOBIOLOGICA
Vol. 60, No. 1, 2022
pp. 74–88

ORIGINAL PAPER

VIA MEDICA

Insulin-like growth factor-1 inhibits apoptosis of rat gastric smooth muscle cells under high glucose condition via adenosine monophosphate-activated protein kinase (AMPK) pathway

Xiang-zi Zhang[1, 2], Yan Sun[1], Mo-han Zhang[1*], Zheng Jin[1*]

[1]Yanbian University College of Medicine, Yanji 133000, China
[2]Department of Stomatology, Affiliated Hospital of Yanbian University,Yanji 133000, China

Abstract

Introduction. Diabetic gastroparesis (DGP) is a common chronic complication of diabetes characterized by decreased gastric motility, and an effective number of gastric smooth muscle cells (GSMCs) ensures gastric motility. A previous study documented that apoptosis was present in gastric smooth muscles in rats with DGP and adenosine monophosphate-activated protein kinase (AMPK) was an important factor of apoptosis of rat GSMCs cultured under high glucose conditions. This study aimed to explore the effect of insulin-like growth factor-1 (IGF-1) on apoptosis of high glucose cultured rat GSMCs after silencing of AMPK and elucidate the underlying mechanism.

Material and methods. A total of 120 rats were divided into normal control (NC, n = 20), diabetic gastroparesis (DGP, n = 50) and DGP + IGF-1 (n = 50) groups. After establishing the rat model of DGP, rats in the DGP+IGF-1 group received an intraperitoneal injection of IGF-1 at a dose of 1.5 μg/kg/d for 10 weeks. The level of AMPK activity, liver kinase B1 (LKB1) activity, and calcium/calmodulin-dependent protein kinase β (CaMKKβ) expression in rat gastric smooth muscle tissues was detected by Western blot analysis. Apoptosis in rat gastric smooth muscle tissues was detected by TUNEL assay. We also cultured rat GSMCs *in vitro* under high glucose (HG) condition (35 mM), incubated cells with IGF-1, and silenced AMPK with siRNA. The cells were divided into HG, HG + IGF-1, HG + siRNA, and HG + siRNA + IGF-1 groups. The apoptosis rates of rat GSMCs after silencing AMPK were detected by TUNEL assay and flow cytometry, and apoptosis-related protein expression in rat GSMCs was detected by Western blot.

Results. IGF-1 decreased LKB1 activity, CaMKKβ expression, AMPK activity, and inhibited apoptosis in rat gastric smooth muscle tissues. Compared with rat GSMCs cultured *in vitro* under HG conditions, apoptosis rates were reduced after treatment with IGF-1 and AMPK silencing (both $p < 0.01$). Apoptosis rates were higher in the HG + siRNA group compared with the HG + IGF-1 group ($p < 0.05$). IGF-1 down-regulated the expression of calcium/calmodulin-dependent kinase II (CaMKII) and p53, up-regulated the expression of p21, PLC-β_3, PI3K p110 Ser^{1070}, and the activities of Akt, p70S6K, mTORC1, and mTORC2. IGF-1 also up-regulated Bcl-2 expression and down-regulated the expression of BAX and Caspase-3.

Conclusions. IGF-1 can inhibit the apoptosis of rat GSMCs under high glucose conditions, its mechanism may be related to the regulation of expression and activity of p53, PI3K, TSC-2, Akt, mTOR, 4E-BP1, p70S6K, p21, CaMKII, and PLC-β3 in rat GSMCs acting through AMPK pathway. *(Folia Histochemica et Cytobiologica 2022, Vol. 60, No. 1, 74–88)*

Key words: rat; gastric smooth muscle cells; IGF-1; high glucose; apoptosis; AMPK signaling; siRNA

Correspondence adresse: Mo-han Zhang,
Yanbian University College of Medicine, Yanji 133000, China
e-mail: mhzhang@ybu.edu.cn
Zheng Jin,
Yanbian University College of Medicine, Yanji 133000, China
e-mail: jinzheng@ybu.edu.cn

Folia Histochem Cytobiol. 2022
10.5603/FHC.a2022.0005
ISSN 0239-8508, e-ISSN 1897-5631

www.journals.viamedica.pl/folia_histochemica_cytobiologica

Introduction

Diabetic gastroparesis (DGP) is manifested by gastric dysmotility [1]. The specific pathogenesis is not yet known, but long-term high blood glucose levels are the cause of DGP. Although the contraction of gastric smooth muscle cells (GSMCs) in the body is regulated by neural and humoral factors [2], the related changes in GSMCs themselves are also factors that should not be ignored. Apoptosis refers to the autonomous programmed death of cells that is controlled by genes in order to maintain the stability of the internal environment, which has become a research hotspot in various biological fields [3]. Apoptosis is an important factor affecting the number of functional cells and an increased apoptosis rate can reflect a greater proportion of apoptotic cells. A previous study documented the existence of spontaneous contraction disorders and apoptosis in gastric smooth muscles in DGP rats [4], and the authors suggested that high glucose serum concentration can induce apoptosis of GSMCs and participate in the occurrence of gastric dysmotility. Finding effective interventions to suppress apoptosis of rat GSMCs cultured under high glucose (HG) conditions is undoubtedly positive for the prevention of DGP and other complications of diabetes.

Under HG conditions (glucose concentration in cell culture medium > 30 mM), cell apoptosis can be regulated by a variety of cytokines and signaling pathways [5, 6]. Adenosine monophosphate-activated protein kinase (AMPK) is a heterotrimer composed of a catalytic subunit (α) and two regulatory subunits (β and γ) [7]. Phosphorylation of AMPK is required for AMPK activity. Phosphorylation at T172 of the α-subunit is a key way to regulate AMPK activity. Our previous animal experiment [4] found that AMPK activity first decreased and then increased in rat GSMCs cultured under HG condition, moreover, *in vitro* experiment confirmed that AMPK promoted the apoptosis of rat GSMCs cultured in HG concentration at the early stages, the effect was not obvious; but with prolonged exposure to high glucose, AMPK was the pro-apoptotic factor. Thus, the results indicated that high glucose concentration can induce apoptosis by regulating AMPK activity [4]. Insulin-like growth factor (IGF-1) is a polypeptide similar in structure to insulin. IGF-1 acts in endocrine, autocrine, and paracrine modes, and plays an important role in cell proliferation and differentiation [8]. IGF-1 has an inhibitory effect on apoptosis of endothelial cells after spinal cord injury [9]. Moreover, IGF-1 can also regulate the biological activity of AMPK [10, 11]. However, the effects of IGF-1 on AMPK activity and AMPK-mediated apoptosis of GSMCs under high glucose conditions and the underlying mechanisms have yet not been reported.

In the present study, we established a rat model of DGP, observed the effect of IGF-1 on the spontaneous contraction of gastric smooth muscle, as well as its effect on AMPK activation and apoptosis in rat gastric smooth muscle tissues. We also cultured rat GSMCs under high glucose conditions, observed the apoptosis of rat GSMCs after silencing AMPK, explored whether IGF-1 regulates apoptosis through AMPK, detected the phosphorylation changes in the AMPK signaling pathway by using AMPK Signaling Phospho-Antibody Array, identified apoptosis-related proteins. The purpose of this study is to elucidate the possible mechanism of action of IGF-1 in DGP and to provide a scientific theoretical, and experimental basis for the exploration of new treatment options for DGP.

Materials and methods

Materials. The following reagents were purchased: streptozotocin (STZ) (No. S0130, Sigma, St. Louis, MO, USA), IGF-1 (No. REGFP-0901, Cyagen Biosciences, Inc., Santa Clara, CA, USA), TUNEL apoptosis detection kit (No. 4030ES50, Yeasen Biotechnology Co., Ltd., Shanghai, China), hematoxylin and eosin (HE) staining kit (Cat. No. G1120, Solarbio Science and Technology Co., Ltd., Beijing, China), Apoptosis detection kit (No. 556547, BD Biosciences, Heidelberg, Germany), Rat GSMCs (NO. RAT-iCell-d005, iCell, Shanghai, China), primary smooth muscle cell low serum culture system (No. PriMed-iCell-004, iCell Bioscience, Shanghai, China), lentivirus-expressed small interfering RNA (siRNA, AMPKα1+α2, Genepharma, Suzhou, China), the protein antibody array (No. PAM174, Full Moon BioSystems, Sunnyvale, CA, USA), phospho (p)-AMPK Thr^{172} antibody (No. ab133448, Abcam, Cambridge, UK), AMPK antibody (No. ab131512, Abcam), liver kinase B1 (LKB1) antibody (No. 3047, Cell Signaling Technology, Danvers, MA, USA), phospho (p)-LKB1 Ser^{428} antibody (No. 3482, Cell Signaling Technology), calcium/ /calmodulin-dependent protein kinase β (CaMKKβ) antibody (No. ab96531, Abcam), calcium/calmodulin-dependent kinase II (CaMKII) antibody (No. ab52476, Abcam), p53 antibody (No. 32532, Cell Signaling Technology), p21 antibody (No. ab80633, Abcam), phospholipase C-β3 (PLC-β3) antibody (No. 14247, Cell Signaling Technology), phospho (p)-phosphoinositide 3-kinase (PI3K) p110 Ser^{1070} antibody (No. bs-6417R, BIOSS Biological Technology. Co. Ltd, Beijing, China), protein kinase B (Akt) antibody (No. 9272, Cell Signaling Technology), phospho (p)-Akt Ser^{473} antibody (No. 4060, Cell Signaling Technology), mechanistic target of rapamycin (mTOR) antibody (No. 2792, Cell Signaling Technology), phospho (p)-mTOR Ser^{2448} antibody (SAB4504476, Sigma), phospho (p)-mTOR Ser^{2481}

Folia Histochem Cytobiol. 2022
10.5603/FHC.a2022.0005
ISSN 0239-8508, e-ISSN 1897-5631

antibody (SAB4301526, Sigma,), eukaryotic translation initiation factor 4E (eIF4E)-binding protein 1 (4E-BP1) antibody (No. 9452, Cell Signaling Technology), p70 ribosomal protein S6 kinase (p70S6K) antibody (No. 9202, Cell Signaling Technology), phospho (p)-p70S6K Thr^{389} antibody (No. 9205, Cell Signaling Technology), B-cell lymphoma 2 (Bcl-2) antibody (No. ab196495, Abcam, Cambridge, UK), Bcl-2-associated X protein (Bax) antibody (No. ab32503, Abcam), Caspase-3 antibody (No. ab4051, Abcam), β-actin antibody (A5316, Sigma).

Animals, the diabetic gastroparesis model, and experimental groups. One hundred and twenty male adult Sprague Dawley rats, weighing 200 ± 20 g, were provided by the Experimental Animal Center of Yanbian University. All animal experimental procedures were approved by the Ethics Committee of Yanbian University College of Medicine.

0.5% STZ solution was prepared in 0.1 mol/L citrate buffer (pH 4.0). Rats were housed in a room with a temperature of 20°C, relative humidity of 60%, and a 12-hr light: dark cycle.

They had free access to food and water and were adapted to the environment for 1 week. Rats were fasted for 12 h before weighing and administration of a single intraperitoneal injection of 65 mg/kg 0.5% STZ. The animals had free access to water throughout the experiment. Seven days after injection, blood samples were collected *via* the tail vein. Blood glucose concentration was measured by OneTouch Verio Reflect™ system (LifeScan, Wayne, PA, USA). Blood glucose levels > 350 mg/dl (19.45 mM) indicated the successful establishment of STZ-induced diabetes. According to the results from our previous study, DGP was developed at 6 weeks after the establishment of the diabetic rat model [4, 12].

One hundred rats with DGP were selected and divided into DGP and DGP + IGF-1 groups with 50 rats *per* group, and 20 untreated, normal rats were chosen as normal control (NC) group. Rats in the DGP + IGF-1 group received an *i.p.* injection of IGF-1 at a dose of 1.5 μg/kg/d for 10 weeks, and rats in the DGP and NC groups received an *i.p.* injection of the same dose of normal saline for 10 weeks.

Detection of morphological changes in gastric smooth muscle tissues by HE staining. Eight rats each from the NC and DGP and DGP + IGF-1 groups were randomly selected and euthanized after a 24 h fast. Then, the whole stomach was rapidly excised, the gastric smooth muscle tissues were fixed in Bouin's fluid (25 ml of 40% formaldehyde, 75 ml of saturated aqueous picric acid, 5 ml of glacial acetic acid) for 12 hours, dehydrated, and infiltrated with paraffin wax. The infiltrated tissues were then embedded into paraffin blocks. Paraffin blocks were cut into 7 μm-thick sections at room temperature (RT). After dewaxing, the section was stained with HE to observe the changes of gastric smooth muscle tissues of rats in each group.

Detection of changes in the spontaneous contraction of isolated gastric smooth muscle. Eight rats each from the NC, DGP, and DGP + IGF-1 groups were randomly selected and euthanized after a 24 h fast. The whole stomach of rats was taken and cut along the lesser curvature, the contents of the stomach were washed out in oxygen-saturated Kreb's solution at 4°C. Circular muscle strips of the antrum (2 mm × 12 mm) were dissected. Strip was attached to an isometric tension transducer in Kreb's solution, the solution was maintained at 37°C and bubbled continuously with a mixture of 95% O_2 and 5% CO_2. Upon the experiment, strips were preloaded with 0.25 g and incubated for 40 min. After stabilization of spontaneous contractions of the strips, the smooth muscle contraction was recorded simultaneously using a four-channel physiological signal recording system (RM6240, Chengdu Instrument Factory, Chengdu, China). Care was taken to prevent the adhesion of the strips.

Detection of the expression of p-AMPK Thr^{172}, AMPK, p-LKB1 Ser^{428}, LKB1, CaMKKβ in rat gastric smooth muscle tissues by Western blot analysis. Eight rats each from the DGP and DGP + IGF-1 groups were randomly selected and euthanized after a 24 h fast, then the whole stomach was excised. Gastric smooth muscle tissues were placed in a 1.5 mL centrifuge tube. 100 µl of ice-cold RIPA lysis buffer containing 1 mM PMSF was added for 10 mg of tissue. Then the samples were homogenized on ice using a handheld homogenizer (MT-30k, Hangzhou Mioyi Instrument Co., Ltd., Hangzhou, China) and centrifuged at 12,000 *g* for 5 min at 4°C. Total proteins were then extracted and protein concentrations were determined using a BCA protein assay kit (cat. no. PC0020, Beijing Solarbio Science & Technology Co., Ltd., Beijing, China). Proteins were boiled for 2 min, and 40 µg of proteins were loaded into each well. After separation of the proteins by electrophoresis in 10% polyacrylamide gel, the proteins were transferred to polyvinylidene difluoride membrane. The membranes were blocked with 5% skimmed milk powder in TBS-T buffer solution. After the blocked membranes were washed, they were incubated with primary antibodies, p-AMPK Thr^{172} (1:1,000), AMPK (1:1,000), p-LKB1 Ser^{428} (1:1,000), LKB1 (1:1,000), CaMKKβ (1:1,000), and β-actin (1:500) at 4°C overnight. After washing the membranes, they were incubated with HRP conjugated goat anti-rabbit IgG secondary antibody for 1 h at RT. Then the membranes were washed and exposed, and β-actin was used as the internal reference.

Detection of apoptosis in gastric smooth muscle tissues by TUNEL assay. Eight rats each from the DGP and DGP + IGF-1 groups were randomly selected and euthanized after a 24 h fast. Then the whole stomach was rapidly excised, the gastric smooth muscle tissues were fixed, dehydrated,

Folia Histochem Cytobiol. 2022
10.5603/FHC.a2022.0005
ISSN 0239-8508, e-ISSN 1897-5631

infiltrated with paraffin wax, and embedded in a paraffin block. Paraffin block was cut into 7 μm-thick sections at RT. After dewaxing, apoptosis was detected by using TUNEL Apoptosis Detection Kit according to the manufacturer's instructions. Five fields at the magnification of 200× were randomly selected from each section and apoptotic cells were observed under a fluorescence microscope (Cytation 5 Cell Imaging Microplate Detection System, BioTek Instruments, Inc., Winooski, VT, USA), green fluorescence in the nucleus indicated TUNEL-positive apoptotic cells. The fluorescence intensity was quantitatively analyzed using Image-Pro Plus 6.0 (Media Cybernetics, Inc., Rockville, MD, USA).

Silencing of AMPK with siRNA. The deep-frozen rat gastric smooth muscle cells purchased from iCell Bioscience Inc (Shanghai, China) were recovered and cultured in primary smooth muscle cell low serum (10%) culture system (iCell Bioscience) and passaged 2–3 times. Rat GSMCs in the logarithmic growth phase were obtained, digested with trypsin (2.5%), and resuspended in primary smooth muscle cell low serum culture system. 1×10^6 of cells were added into a 24-well plate and incubated at 37°C overnight. The solution containing siRNA-expressing lentiviral vectors (AMPKα1 + α2) was mixed and diluted with the primary smooth muscle cell low serum culture system in a 1:2 ratio, the total volume was 500 µl. The old medium was aspirated from the plate, lentiviral dilutions were added, and after incubation at 37°C for 24 h, the medium was aspirated and replaced with 1 mL of fresh medium. After incubation at 37°C for 72 h, the cells were observed and photographed under a fluorescence inverted microscope. Cells were collected for subsequent experiments when transfection efficiency reached > 70%. Transfection efficiency was determined by monitoring the expression of green fluorescent protein using fluorescence microscopy.

Detection of the apoptosis rates of rat GSMCs after silencing AMPK by flow cytometry. After recovering the primary rat GSMC line, cells were passaged 2–3 times. Cell density was adjusted to 1×10^6/ml. Then cells were divided into HG (35 mmol/L) and HG + IGF-1 (100 ng/ml) groups. The IGF-1 concentration of 100 ng/ml was determined by prior dose-response experiments. After silencing AMPK in rat GSMCs, cells were passaged 1 to 2 times, and the cell density was adjusted to 1×10^6/ml. Then cells were divided into HG + siRNA and HG + siRNA+IGF-1 groups. Flow cytometry was performed at 48 h of culture to detect the apoptosis rates of rat GSMCs. The experiments were repeated at least 3 times.

Detection of the changes in the AMPK pathway by using protein antibody arrays. After culturing cells for 48 hours, the protein antibody array was performed to detect the changes in the AMPK pathway in the HG and HG + IGF-1 groups. Proteins were extracted according to the kit instructions. Apoptosis-related proteins in the AMPK pathway were identified.

Detection of apoptosis-related protein expression in rat GSMCs by Western blot analysis. Rat GSMCs in the logarithmic growth phase were obtained, divided into HG and HG + IGF-1 groups, and cultured for 48 h. The procedures of Western blot were the same as those mentioned above. Antibodies were CaMKII (1:1,000), p53 (1:1,000), PLC-β_3 (1:1,000), p21 (1:1,000), PI3K p110 Ser^{1070} (1:500), Akt (1:1,000), p-Akt Ser^{473} (1:1,000), 4E-BP1 (1:1,000), p70S6K(1:1,000), p-p70S6K Thr^{389} (1:1,000), p-mTOR Ser^{2448} (1:500), p-mTOR Ser^{2481} (1:500), mTOR (1:1,000), Bcl-2 (1:1,000), BAX(1:1,000), Caspase-3(1:1,000), β-actin (1:500). The experiments were repeated at least 3 times.

Statistical analysis. Statistical analyses were performed with SPSS 21.0 software (IBM Co., Armonk, NY, USA). All figures were drawn using GraphPad Prism5 software (GraphPad Inc., San Diego, CA, USA). Data are expressed as mean ± standard error of the mean (SEM). Differences between groups were compared using a *t*-test and two-way analysis of variance (ANOVA). $p < 0.05$ was considered to indicate a significant difference, $p < 0.01$ was considered to indicate a highly significant difference.

Results

Comparison of blood glucose concentrations and body weight between groups

The body weight of rats in the DPG group was lower than in normal control (NC) rats (174.8 ± 3.26 g *vs.* 219.0 ± 5.18 g, respectively, $p < 0.01$), and the blood glucose concentration of rats in the DPG group was higher than in the NC group (28.46 ± 1.47 mM *vs.* 7.01 ± 0.28 mM, respectively, $p < 0.01$).

After treatment with IGF-1, the body weight of rats in the DGP+IGF-1 group was higher than the DGP group (197.4 ± 3.17 g *vs.* 174.8 ± 3.26 g, $p < 0.01$), and lower than the NC group (197.4 ± 3.17 g *vs.* 219.0 ± 5.18 g, $p < 0.01$). The blood glucose concentrations of rats in the DGP + IGF-1 group were lower than the DGP group (10.26 ± 0.69 mM *vs*. 28.46 ± 1.47 mM, $p < 0.01$), and higher than the NC group (10.26 ± 0.69 mM *vs.* 7.01 ± 0.28 mM, $p < 0.05$, Fig. 1).

Morphological changes of gastric smooth muscle tissues in each group

HE staining showed that in the NC group, gastric smooth muscles were arranged regularly and tightly, with moderate intercellular gaps, and did not present vacuolar degeneration. In the DGP group, the cyto-

10.5603/FHC.a2022.0005
ISSN 0239-8508, e-ISSN 1897-5631

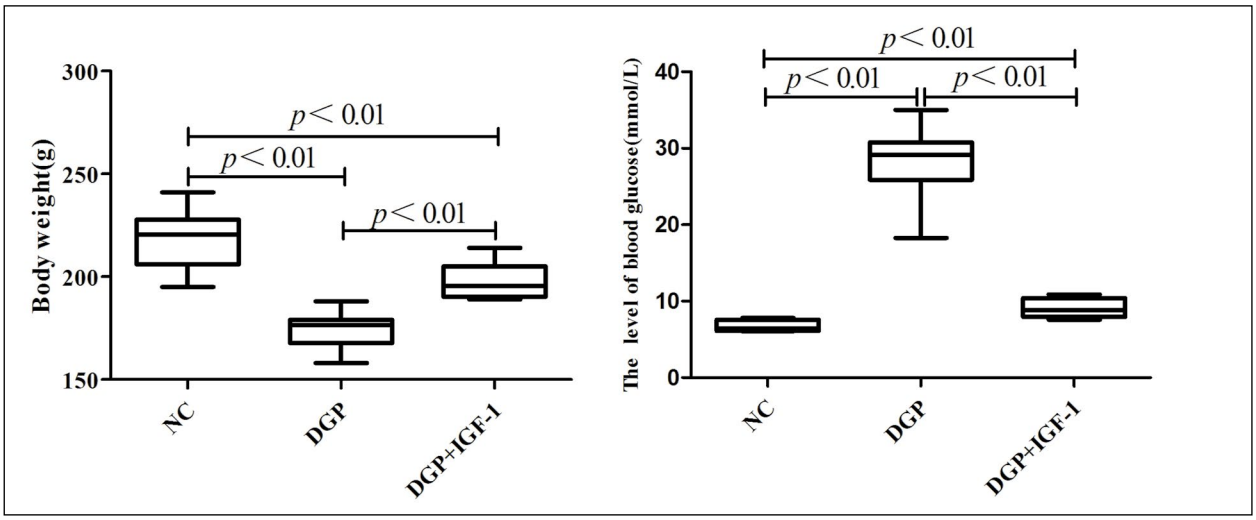

Figure 1. The effect of IGF-1 (1.5 μg/kg/d, *i.p.*, 10 weeks) on body weight and blood glucose levels of streptozotocin-induced diabetic gastroparesis (DGP) rats. NC — control rats; DGP + IGF-1 — DGP rats that received IGF-1. Data are expressed as mean ± SEM, n = 8 *per* group.

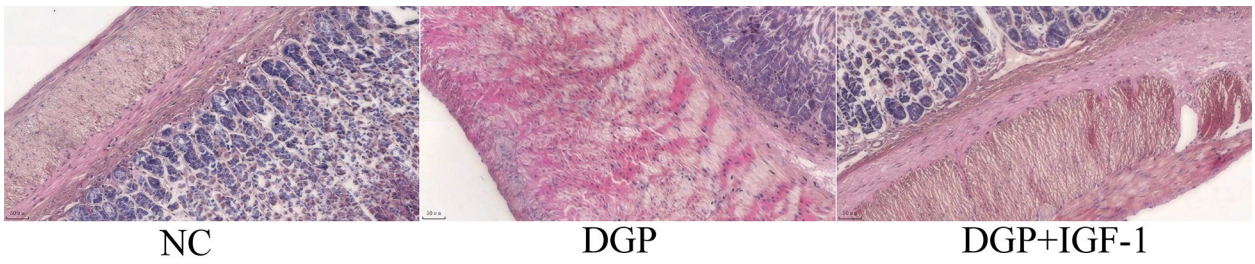

Figure 2. The effect of IGF-1 (1.5 μg/kg/d, *i.p.*, 10 weeks) on the morphological changes of gastric smooth muscle tissues of DGP rats. Magnification: 200×. N = 8 *per* group. Abbreviations as in the description of Fig. 1.

plasm of the gastric smooth muscle was lightly stained and translucent, vacuolar degeneration was observed. In the DGP + IGF-1 group, gastric smooth muscles were arranged regularly with fewer vacuoles (Fig. 2).

Changes in the spontaneous contraction of gastric smooth muscle between groups

The frequency and amplitude of spontaneous contraction of gastric smooth muscles were both lower in the DGP group than that in the NC group (13.82 ± 0.46 *per* sec *vs.* 29.52 ± 1.06 *per* sec, $p < 0.05$; 0.41 ± 0.02 *vs.* 0.90 ± 0.05, frequency and amplitude, respectively, $p < 0.01$). After treatment with IGF-1, the frequency of spontaneous contractions in the DGP + IGF-1 was lower than that in the NC group (20.08 ± 0.85/sec *vs.* 29.52 ± 1.06/sec, $p < 0.01$), and was higher than in the DGP group (20.08 ± 0.85/sec *vs.* 13.82 ± 0.46/sec, $p < 0.01$). The amplitude of spontaneous contractions in DGP + IGF-1 group was reduced as compared with the NC group (0.62 ± 0.05 *vs.* 0.90 ± 0.05, $p < 0.01$), and higher as compared with the DGP group (0.62 ± 0.05 *vs.* 0.41 ± 0.02, $p < 0.01$, Fig. 3).

Changes in the levels of LKB1, AMPK activities, and CaMKKβ expression in rat gastric smooth muscle tissues between groups

Ratio of phospho-AMPK Thr^{172}/AMPK and phospho-LKB1 Ser^{428}/LKB1 were both higher in the DGP group than that in the DGP + IGF-1 group (0.92 ± 0.06 *vs.* 0.77 ± 0.03, $p < 0.05$; 0.83 ± 0.05 *vs.* 0.61 ± 0.04, $p < 0.05$, respectively). CaMKKβ expression was increased in the DGP group than that in the DGP + IGF-1 group (0.68 ± 0.04 *vs.* 0.50 ± 0.03, $p < 0.01$, Fig. 4).

Changes in apoptosis in rat gastric smooth muscle tissues between groups

The nuclei of TUNEL-positive cells exhibited green fluorescence, the results showed that significantly more TUNEL-positive nuclei were found in the DGP

Folia Histochem Cytobiol. 2022
10.5603/FHC.a2022.0005
ISSN 0239-8508, e-ISSN 1897-5631

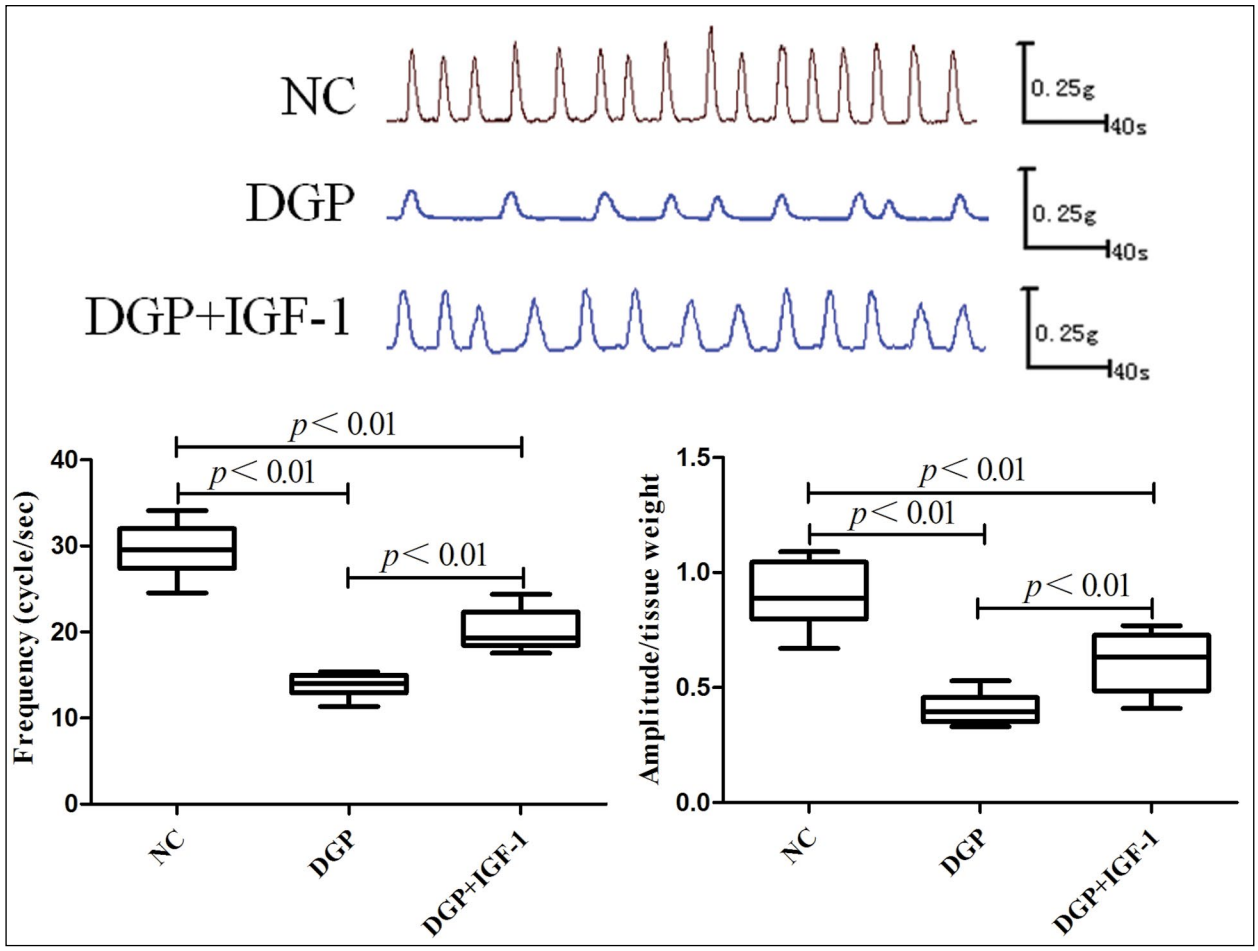

Figure 3. The effect of IGF-1 (1.5 μg/kg/d, *i.p.*, 10 weeks) on the frequency and amplitude of spontaneous contractions of gastric smooth muscle DGP rats. Data are expressed as mean ± SEM, n = 8 *per* group. Abbreviations as in the description of Fig. 1.

group *versus* the DGP + IGF-1 group (90.05 ± 1.77 *vs.* 68.72 ± 2.44, $p < 0.01$, Fig. 5).

Effects of silencing of AMPK with siRNA

The lentiviral transfection efficiency for cells was more than 70% (Fig. 6A). After adding 5-aminoimidazole-4-carboxamide1-β-D-ribofuranoside (AICAR), the expression of phospho-AMPK Thr^{172} was higher in the NC+AICAR group compared with the NC group (0.85 ± 0.04 *vs.* 0.48 ± 0.02; $p < 0.01$), and phospho-AMPK Thr^{172} expression was not significantly changed after transfection with AMPK α1/α2 siRNA (Fig. 6B). After the cells were transfected with lentivirus-expressed siRNA (AMPKα1+α2), the AMPKα expression was higher in the NC group compared with the siRNA group (1.57 ± 0.02 *vs.* 0.25 ± 0.02; $p < 0.01$), indicating that AMPKα expression was significantly inhibited (Fig. 6C).

Effects of IGF-1 on the apoptosis of rat GSMCs after silencing AMPK

GSMCs were incubated with or without IGF-1 (100 ng/ml). Apoptosis rates were higher in the GSMCs cultured under HG condition compared with the HG + IGF-1 group (7.96 ± 0.04% *vs.* 5.71 ± 0.13%, $p < 0.01$) as well as the HG + siRNA group (7.96 ± 0.04 *vs.* 6.59 ± 0.16, $p < 0.01$). Apoptosis rates were higher in the HG + siRNA group compared with the HG + IGF-1 group (6.59 ± 0.16 *vs.* 5.71 ± 0.13, $p < 0.05$). There were no statistically significant differences between the HG + siRNA + IGF-1 and HG + IGF-1 groups (Fig. 7).

Effect of IGF-1 on changes in AMPK signaling pathway in rat GSMCs cultured under high glucose conditions

GSMCs were incubated with or without IGF-1 (100 ng/ml). All target proteins were normalized to internal

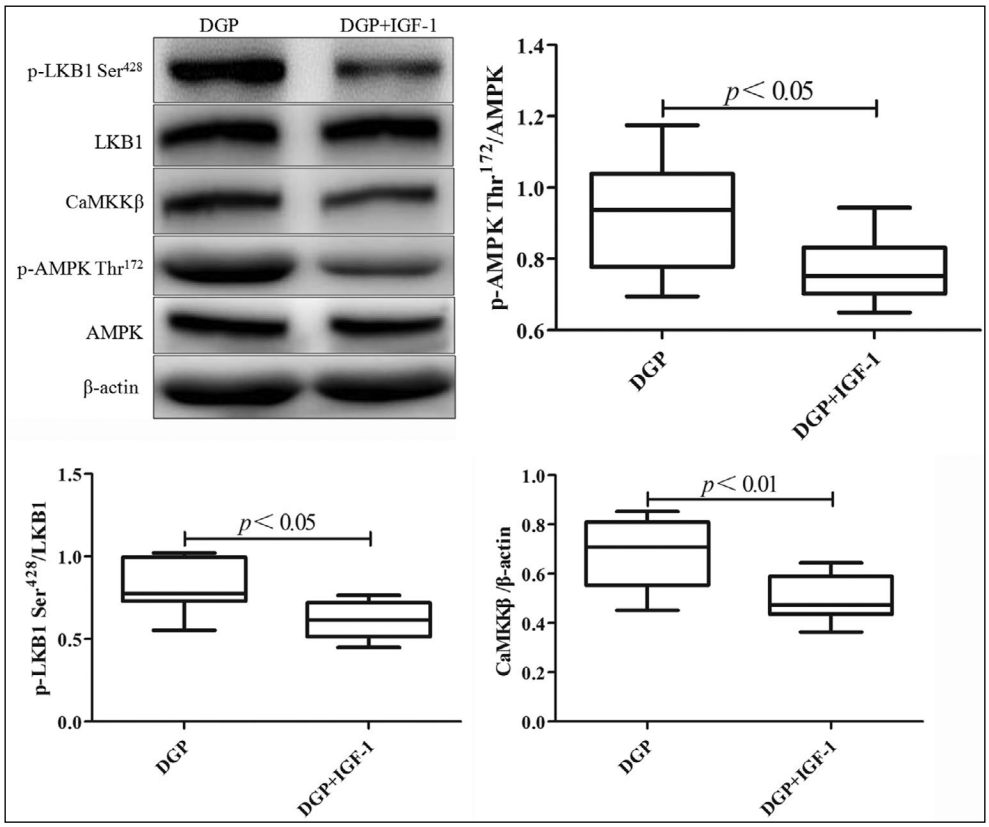

Figure 4. The effect of IGF-1 (1.5 μg/kg/d, *i.p,* 10 weeks) on the activities of LKB1, AMPK, and the expression of CaMKKβ in the gastric smooth muscle of DGP rats. Data are expressed as mean ± SEM, n = 8 per group. Abbreviations as in the description of Fig. 1.

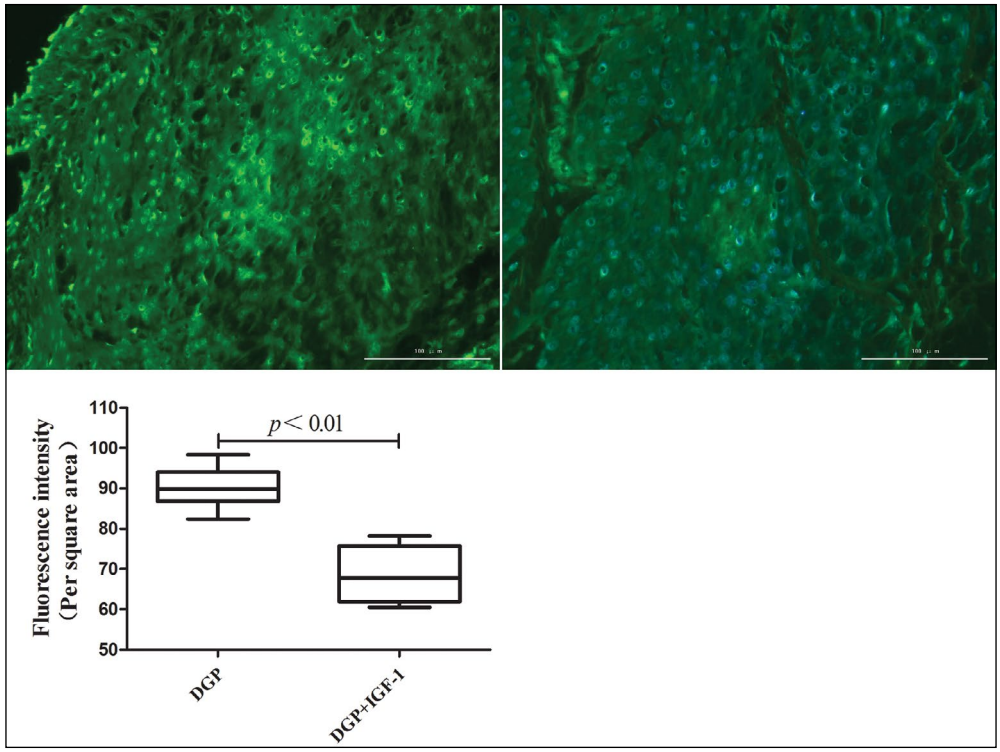

Figure 5. Effect of IGF-1 (1.5 μg/kg/d, *i.p.*, 10 weeks) on the apoptosis in gastric smooth muscle tissues of DGP rats. Data are expressed as mean ± SEM, n = 8 per group. The nuclei of apoptotic cells exhibited green TUNEL. Magnification: 200×. Abbreviations as in the description of Fig. 1.

Folia Histochem Cytobiol. 2022
10.5603/FHC.a2022.0005
ISSN 0239-8508, e-ISSN 1897-5631

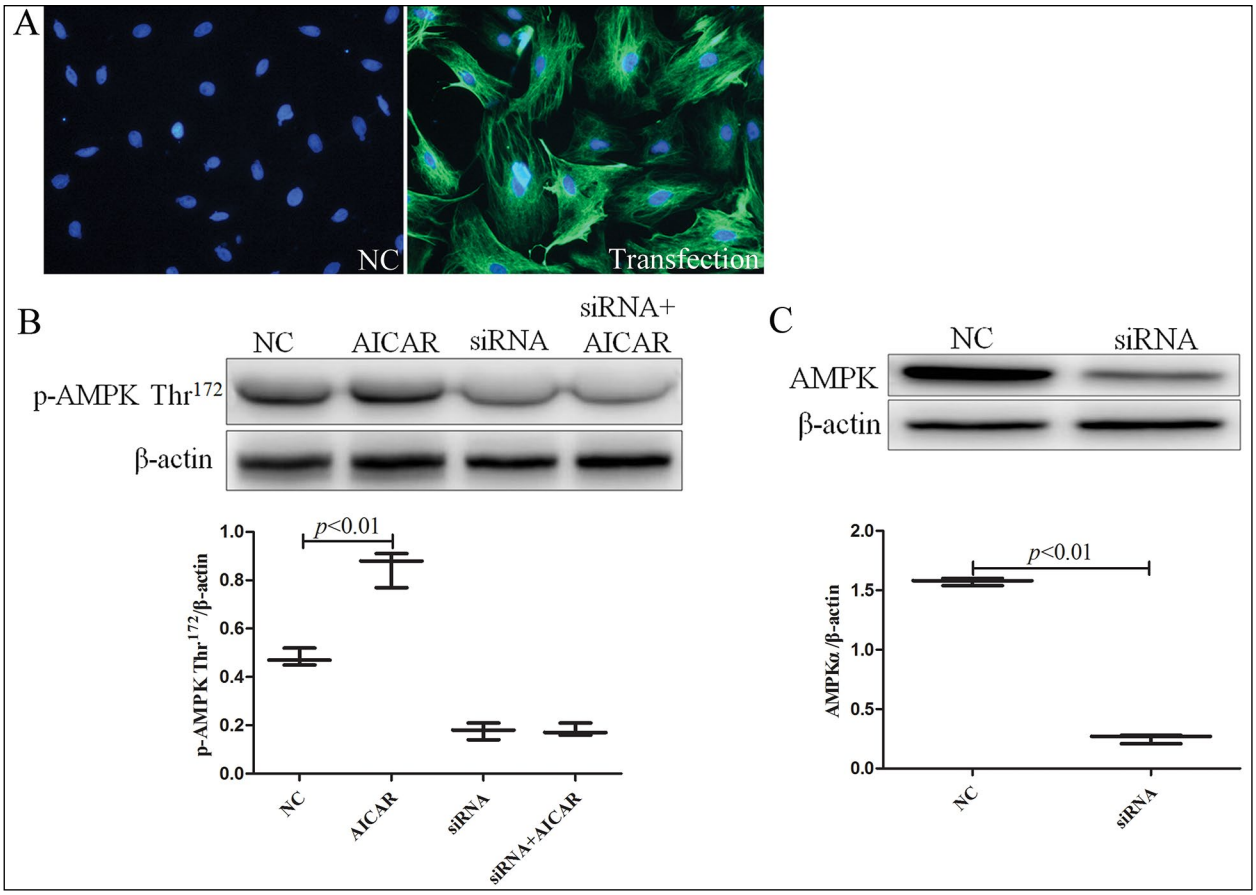

Figure 6. Effect of silencing of AMPK with small interfering RNA in rat gastric smooth muscle cells. **A.** Transfection efficiency of lentiviral after 72 h of transfection (magnification: 200×). **B.** Changes in AMPK Thr^{172} phosphorylation after silencing AMPK and adding 5-aminoimid-azole-4-carboxamide1-β-D-ribofuranoside (AICAR). **C.** Expression of AMPKα in NC (control) and siRNA groups after silencing AMPK. The experiment was repeated three times independently.

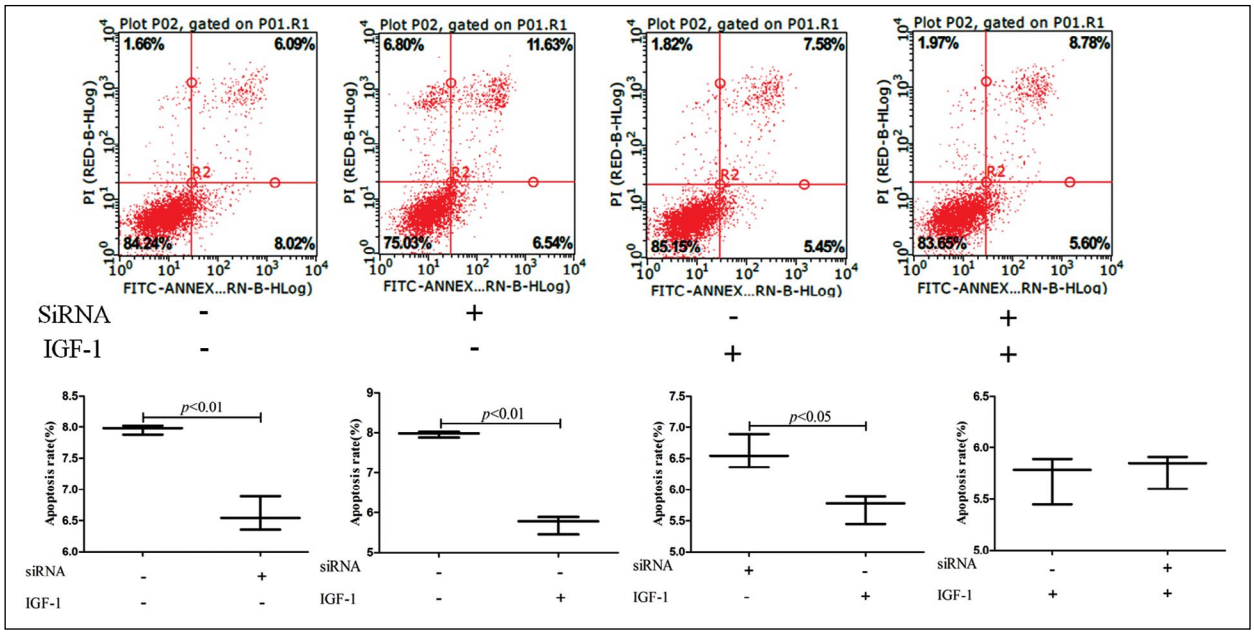

Figure 7. Effects of IGF-1 (100 ng/ml) on apoptosis of high glucose (35 mM)-cultured rat gastric smooth muscle cells after silencing of AMPK measured by flow cytometry as described in Methods. The experiment was repeated three times independently.

Folia Histochem Cytobiol. 2022
10.5603/FHC.a2022.0005
ISSN 0239-8508, e-ISSN 1897-5631

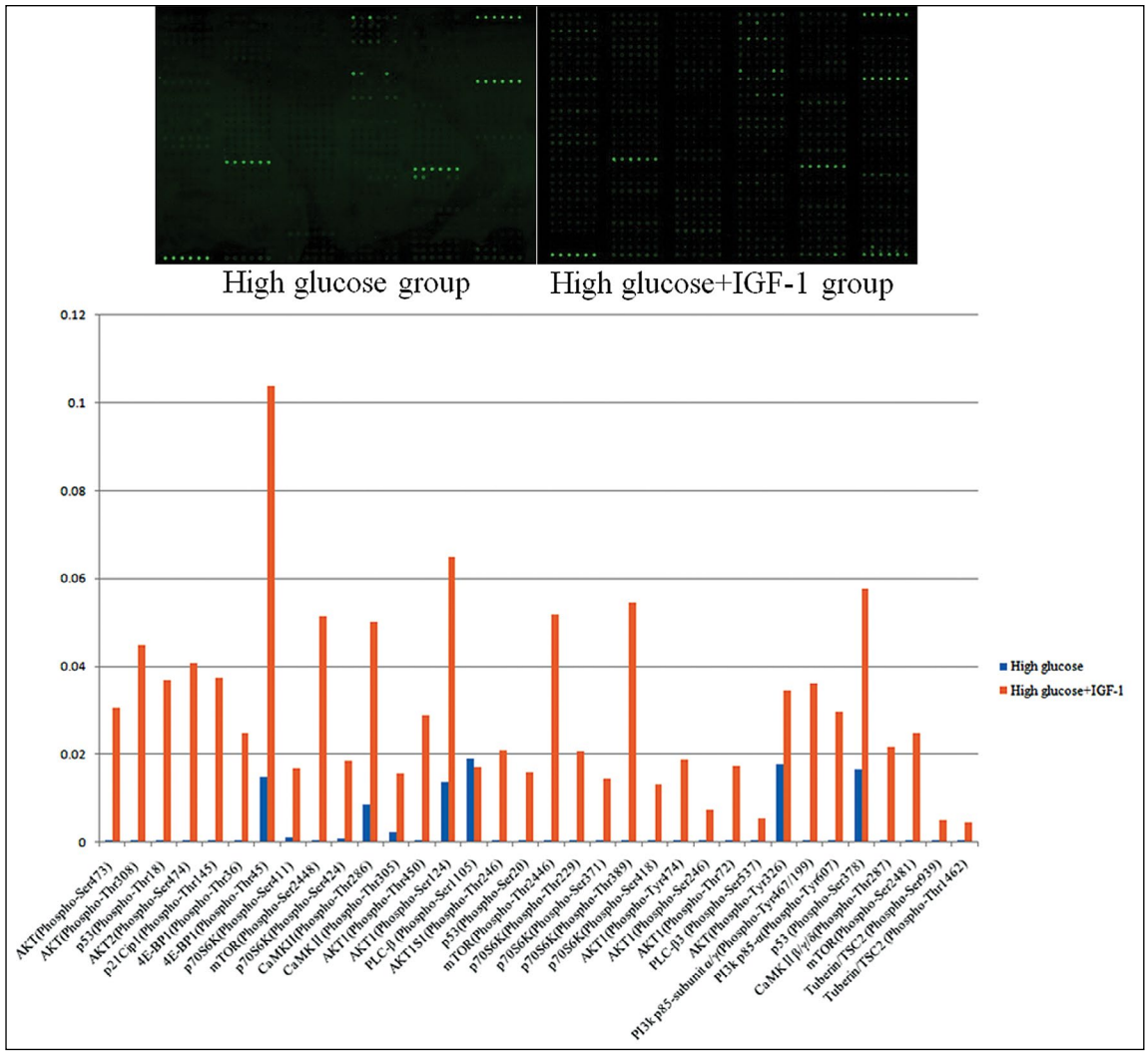

Figure 8. Effect of IGF-1 (100 ng/ml) on changes in the AMPK signaling pathway in rat gastric smooth muscle cells cultured under high glucose concentration (35 mM). The experiment was repeated three times independently.

reference β-actin (*i.e.* dividing the signal intensity of the target protein with that of β-actin). Fold change ≥ 1.5 was used as inclusion criteria for differentially expressed proteins. A total of 34 differentially phosphorylated sites were identified, including 10 apoptosis-related proteins, p53, PI3K, Akt, tuberous sclerosis complex 2 (TSC-2), mTOR, 4E-BP1, p70S6K, p21, CaMKII, and PLC-β3 (Fig. 8).

Effect of IGF-1 on the expression of apoptosis--related proteins in rat GSMCs cultured under high glucose conditions

P53 and CaMKII expression were increased in the HG group compared with the HG + IGF-1 group (1.05 ± 0.02 *vs.* 0.88 ± 0.03, $p < 0.01$; 0.92 ± 0.08 *vs.* 0.57 ± 0.02, $p < 0.05$, respectively), while p21 and PLC-β_3 and PI3K p110 Ser^{1070} expression and the ratio of p-Akt Ser^{473}/Akt ratio were decreased in the HG group compared with the HG + IGF-1 group (0.55 ± 0.10 *vs.* 0.93 ± 0.07, $p < 0.05$; 1.03 ± 0.04 *vs.* 1.43 ± 0.12, $p < 0.05$, 0.57 ± 0.11 *vs.* 0.92 ± 0.02, $p < 0.05$; 0.37 ± 0.01 *vs.* 1.30 ± 0.25, $p < 0.05$, respectively, Fig. 9A).

4E-BP1 and Bcl-2 expression and the ratio of p-p70S6K Thr^{389}/p70S6K and p-mTOR Ser^{2448}/mTOR and p-mTOR Ser^{2481}/mTOR were decreased in the HG group compared with the HG + IGF-1 group (0.72 ± 0.09 *vs.* 1.06 ± 0.06, $p < 0.05$; 0.33 ± 0.03 *vs.* 0.43 ± 0.02, $p < 0.05$, 0.65 ± 0.08 *vs.* 1.17 ± 0.12, $p < 0.05$; 0.59 ± 0.05 *vs.* 0.97 ± 0.04, $p < 0.01$; 0.48 ± 0.01 *vs.* 1.02 ± 0.02, $p < 0.01$, respectively), while BAX and caspase-3 expression were increased in the HG group compared with the HG + IGF-1 group (0.41 ± 0.01 *vs.* 0.34 ± 0.01, $p < 0.05$; 0.25 ± 0.01 *vs.* 0.17 ± 0.01, $p < 0.01$, respectively, Fig. 9B).

10.5603/FHC.a2022.0005
ISSN 0239-8508, e-ISSN 1897-5631

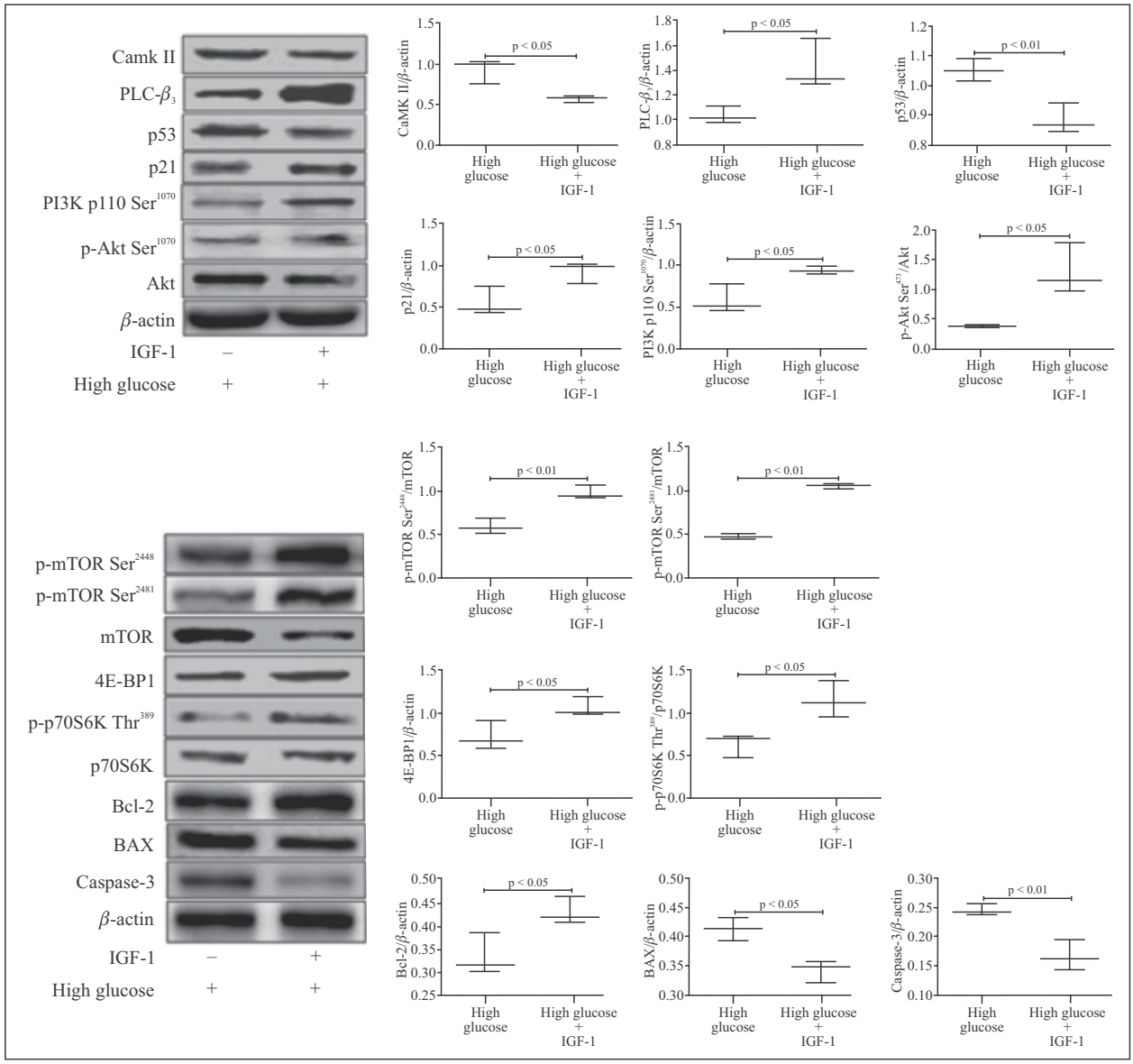

Figure 9. Effect of IGF-1 (100 ng/ml) concentration on the expression of apoptosis-related proteins assessed by Western blotting in rat gastric smooth muscle cells cultured under high glucose concentration (35 mM). The experiment was repeated three times independently.

Discussion

Gastric motility is an important determinant of gastric emptying and an effective number of GSMCs ensures gastric motility. Apoptosis is a common cellular process that can reduce the number of cells. Our previous study [4] demonstrated that gastric motility disorders and apoptosis were present in gastric smooth muscles in rats with DGPS. Because apoptosis is an important cause of gastric motility disorders, the inhibition of apoptosis may play a positive role in ensuring gastric motility. In this study, we found that prolonged administration of IGF-1 improved the morphological structure of rat gastric smooth muscle cells, inhibited the apoptosis in gastric smooth muscle tissues, and increased the amplitude and frequency of spontaneous contractions of gastric smooth muscles in rats with DGP, indicating that inhibition of apoptosis has a significant effect on the recovery of gastric motility. Our previous study [4] documented that AMPK is an important factor of apoptosis of rat GSMCs cultured under high glucose conditions. In this study, we found that IGF-1 inhibited AMPK activity, and the activity of its upstream activator LKB1, as well as CaMKKβ expression. The biological role of CaMKKβ is dependent on intracellular Ca^{2+} levels. A previous study [13]

Folia Histochem Cytobiol. 2022
10.5603/FHC.a2022.0005
ISSN 0239-8508, e-ISSN 1897-5631

found that IGF-1 can down-regulate the Ca^{2+} levels in high glucose-induced rat GSMCs, suggesting that IGF-1 down-regulated AMPK activity by inhibiting the mode of AMPK activation. In this study, in order to investigate whether IGF-1 exerts an inhibitory effect on apoptosis of high glucose-cultured rat GSMCs through the AMPK pathway, we silenced AMPK expression. Our findings showed that under high glucose conditions, IGF-1 inhibited *in vitro* apoptosis through the AMPK pathway. In order to explore the underlying mechanism, we observed the effect of IGF-1 on changes in the AMPK signaling pathway by protein antibody arrays, and out of 34 different phosphorylated sites, 10 involved apoptosis-related proteins.

PI3K has serine/threonine (Ser/Thr) kinase activity, can mediate a wide range of biological functions, including cell endocytosis, exocytosis, and vesicle formation, as well as cell proliferation, differentiation, apoptosis, and glucose transport [14]. PI3K is comprised of a regulatory subunit (p85) and a catalytic subunit (p110). The helical domain of the regulatory subunit p85α/p85β can bind p110, leading to the phosphorylation and activation of p110, followed by recruitment of PI3K to the plasma membrane. The phosphorylation and activation of p110 can also be mediated by G protein-coupled receptors through binding of Ras/Rac to p110 [15]. A previous study [16] showed that AMPK can act as an upstream factor of PI3K to regulate its biological functions in a variety of cells. We demonstrated in this report that under high glucose conditions, IGF-1 can up-regulate the phosphorylation levels of PI3K p85 by inhibiting AMPK activity, which in turn relieves the inhibition of PI3K p110. thereby activating PI3K p110 phosphorylation. This may lead to the up-regulation of the biological activities of PI3K, and inhibition of apoptosis.

Akt is a serine/threonine-specific protein kinase and its activity can be regulated by various upstream factors, including AMPK and PI3K [17, 18]. Akt activation involves the phosphorylation at Thr^{308}, Ser^{473}, which is reflected by the ratio of p-AktSer^{473} to Akt. Activated Akt can cause caspase3 inactivation and inhibit apoptosis [19]. The results of our study showed for the first time that under high glucose conditions, IGF-1 can up-regulate the phosphorylation levels of Akt at ten identified sites and stabilize Akt expression by inhibiting AMPK, which is also involved in inhibiting apoptosis by increasing Akt activity.

TSC-2 is a downstream target of AMPK and also a downstream target of Akt [20, 21]. The biological role of TSC-2 is mainly achieved through its downstream mammalian target of rapamycin (mTOR). TSC-2 can form a heterodimeric complex with TSC-1 (TSC-1/ /TSC-2), TSC-1/TSC-2 complex can inhibit the activity of the upstream protein of mTOR, small GTPase Rheb, thereby inhibiting the binding of Rheb to GTP, and down-regulating mTOR complex 1 (mTORC1) activity [22, 23]. TSC-2 has multiple phosphorylation sites, activated Akt can phosphorylate TSC-2 at Ser^{939} and Thr^{1462}, which in turn inhibits TSC-1/TSC-2 formation and indirectly activates mTORC1 [24]. Activated AMPK can phosphorylate TSC-2 at Ser^{1345} and Ser^{1227}, which directly activates TSC-2 and promotes TSC-1/TSC-2 formation, thereby inhibiting mTORC1 activity. Thus, the biological functions of mTOR are different when the TSC-2 is phosphorylated at different sites [25]. In this study we demonstrated that in rat GSMCs cultured under high glucose conditions, IGF-1 can increase the phosphorylation levels of TSC-2 at Ser^{939} and Thr^{1462} *via* Akt through inhibiting AMPK, thereby suppressing the formation of TSC-1/ /TSC-2 complex, and inhibiting cell apoptosis through activating mTORC1.

The mTOR is an atypical serine/threonine kinase that exists in the form of mTORC1 and mTORC2 complexes [26]. mTORC1 and mTORC2 can sense different nutritional and environmental factors, and participate in the regulation of energy metabolism and cell apoptosis [26]. mTOR is co-regulated by Akt and AMPK and mTOR activity is indicated by its phosphorylation. A study found that mTOR regulated apoptosis of neuroblastoma cells mainly through regulation of its downstream targets p70S6K and 4E- BP1 [27]. Multiple phosphorylation sites are present on mTOR, Ser^{2448} and Ser^{2481} are the phosphorylation sites of mTORC1 and mTORC2, respectively [28]. The results of our study suggest that IGF-1 exerts a regulatory effect on mTOR phosphorylation and expression by inhibiting AMPK, and/or Akt. In this way, IGF-1 may activate mTOR, as well as mTORC1 and mTORC2, respectively, and inhibit cell apoptosis through regulation of p70S6K and 4E-BP1. Interestingly, Sutton and Coran showed in a rat model of cocaine-induced nucleus accumbens sensitization and reward study data suggesting that it reduced the phosphorylation of mTOR at Ser^{2448} by phosphorylating mTOR at Thr^{2446} and inhibited the mTORC1 activity, findings contrary to our results [29]. The differences in the *in vitro* model, cell type, and culture conditions may be responsible for the discrepancy between theirs and our results.

P70S6K is a downstream substrate of mTOR and can be activated by PI3K-Akt and protein kinase C pathways. p70S6K is involved in the regulation of transcription and translation, cell proliferation and apoptosis [30]. p70S6K has several phosphorylation sites, p70S6K phosphorylation at Ser^{411}, Ser^{424}, Thr^{421}, Ser^{418}, and Ser^{371} leads to the release p70S6K from C-terminal self-inhibition and facilitate p70S6K acti-

Folia Histochem Cytobiol. 2022
10.5603/FHC.a2022.0005
ISSN 0239-8508, e-ISSN 1897-5631

vation [31]. p70S6K activation requires the phosphorylation of p70S6K, the phosphorylation of p70S6K at Thr^{389} and Thr^{229} are crucial for p70S6K activity, the ratio of p-p70S6K Thr^{389}/p70S6K can reflect p70S6K activity [32, 33]. Activated p70S6K can phosphorylate Bad at Ser^{136} and cause its dissociation from Bcl-2 and Bcl-xL, which exerts an antiapoptotic effect [30]. In this study, results from protein antibody arrays showed that under high glucose conditions, IGF-1 up-regulated in rat GSMCs p70S6K phosphorylation at six sites whereas Western blot analysis showed that IGF-1 stabilized p70S6K expression, indicating that IGF-1 can up-regulate p70S6K phosphorylation and stabilize its expression through inhibiting AMPK, thereby maximizing the activity of p70S6K, and inhibiting apoptosis of high glucose-cultured rat GSMCs.

4E-BP1 is a small-molecular-weight protein that can bind to eIF4E, thereby inhibiting translation initiation. The phosphorylation level of 4E-BP1 is closely related to its biological function, high levels of phosphorylated 4EBP1 promote the dissociation of eIF4E from 4E-BP1, and low levels of phosphorylated 4EBP1enhances the binding of 4E-BP1 to eIF4E [34]. A previous study [35] showed that increasing the level of phosphorylated 4E-BP1 had an inhibitory effect on the apoptosis of rat neural cells. The reason may be that eIF4E promotes the translation of anti-apoptotic proteins after dissociating 4E-BP1 from eIF4E [35]. 4E-BP1 has many phosphorylation sites, phosphorylation of 4E-BP1 at Thr^{36}, Thr^{45}, Ser^{65}, Thr^{70} are associated with the mTOR pathway. Phosphorylation of 4E-BP1 at Thr^{37}, Thr^{46}, Ser^{65}, Thr^{70} promotes its dissociation from eIF4E [36, 37]. In our current study, results from protein antibody arrays and Western blot analysis showed that IGF-1 up-regulated the 4E-BP1 expression in rat GSMCs. The results suggested that IGF-1 can increase the phosphorylation levels of 4E-BP1 ($Thr^{36/45}$), stabilize its phosphorylation at Ser^{65} via mTOR through inhibiting AMPK, thereby maintaining EIF4E/4E-BP dissociation. Our results differ slightly from the findings of the above-mentioned previous studies [36, 37]. The discrepancy between our results and previous reports may be also due to the use of different cell types and culture conditions.

P53 can regulate apoptosis through its downstream targets, Bcl-2, Bax, and Caspase-3 [38]. The p53 protein has many phosphorylation sites, phosphorylation of P53 at Ser^{15}, Ser^{18}, Ser^{20}, Ser^{315}, Ser^{378}, Ser^{366} can promote DNA transcription [39]. In this study, results from protein antibody arrays showed that in rat GSMCs cultured under high glucose conditionIGF-1 up-regulated p53 phosphorylation whereas Western blot analysis showed that IGF-1 down-regulated wild type p53 expression. These results indicated that under high glucose conditions, IGF-1 can increase the phosphorylation of p53 at the 3 identified sites and decrease p53 expression through inhibiting the AMPK pathway, thereby regulating the biological activities of Bcl-2, Bax, and Caspase-3, and inhibiting cell apoptosis.

P21 has GTPase activity and is involved in regulating cell transmembrane signaling, cell proliferation, differentiation, and apoptosis [40]. Studies [41, 42] have revealed that p21 exerts an inhibitory effect on apoptosis, and this effect is dependent on p53. The p21 protein can also exert a pro-apoptotic effect which is not dependent on p53 [40]. The p21 expression can be regulated by upstream factors such as AMPK and Akt [43, 44]. In this study, results from protein antibody arrays and western blot analysis indicate that IGF-1 exerts a regulatory effect on p21 phosphorylation and expression *via* Akt and p53 pathways through inhibiting AMPK, thereby inhibiting the apoptosis of rat GSMCs.

Ca2+ can induce endoplasmic reticulum stress and initiate ER stress-induced apoptosis signaling pathway [45]. PLCβ/IP3/Ca^{2+} is a basic pathway in the PLC pathway [46]. IP3 generation can stimulate Ca^{2+} influx, the release of endoplasmic reticulum and sarcoplasmic reticulum, and increase the cytoplasmic Ca^{2+} levels. PLC-β_3 is one of the PLC subtypes, and is mainly present in the gastrointestinal tract [47]. PLC-β Ser^{1105} is also known as the inhibitory type of PLC, the increase in PLC-β Ser^{1105} expression can inhibit PLC-β_3 activity and expression, phosphorylation of PLC-β_3 at Ser^{537} can promote PLC-β_3 activity and expression [48]. In this study, the obtained results suggested that IGF-1 can up-regulate the phosphorylation of PLC-β_3 (Ser^{537}), stabilize its phosphorylation at Ser^{1105}, increase PLC-β_3 expression by inhibiting AMPK, and can decrease intracellular Ca^{2+} levels and inhibiting cell apoptosis.

Calcium-calmodulin-dependent protein kinase II (CaMKII) is a member of the Ca^{2+}/calmodulin-dependent protein kinase family. CaMKII phosphorylation is required for CaMKII activity [49]. Increased CaMKII activity can cause intracellular Ca^{2+} accumulation and induce apoptosis of gastric cancer cells [50]. Increased levels of phosphorylated CaMK and decreased levels of non-phosphorylated CaMKII cause decreased CaMKII activity [51]. The results of our study showed that IGF-1 down-regulated CaMKII expression in rat GSMCs, suggesting that IGF-1 could increase the phosphorylation of CaMKII at the identified sites and down-regulate CaMKII expression through inhibiting AMPK, thereby inhibiting CaMKII activity, decreasing the intracellular Ca^{2+} levels and suppressing apoptosis.

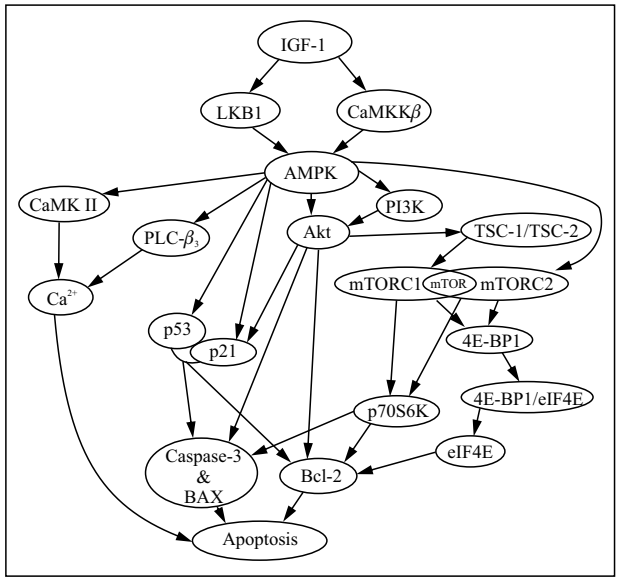

Figure 10. Possible mechanism of IGF-1 effects acting *via* AMPK pathway on inhibiting gastric smooth muscle cell apoptosis under high glucose condition in STZ-induced diabetic rat.

In summary, the results of our study suggest that IGF-1 can inhibit apoptosis in the gastric smooth muscle tissues of DGP rats, which may contribute to the recovery of gastric motility. Moreover, IGF-1 can also inhibit apoptosis of rat GSMCs cultured under high glucose conditions. The inhibitory effect of IGF-1 on apoptosis is mainly achieved by regulating the expression or activity of p53, PI3K, TSC-2, Akt, mTOR, 4E-BP1, p70S6K, p21, CaMKII, and PLC-β_3 through the AMPK pathway as shown in Fig. 10.

Funding

This work was supported by the National Natural Science Foundation of China (grant number 82060154).

Ethics approval

Ethical approval was obtained from the Ethics Committee of Yanbian University College of Medicine.

Statement of informed consent

Not applicable.

Availability of data and materials

All data generated or analyzed during this study are included in this published article.

Authors' contributions

Mo-han Zhang and Zheng Jin designed the study, supervised the data collection, and reviewed the draft of the manuscript; Xiang-zi Zhang wrote the draft of the manuscript, analyzed the data, interpreted the data; Yan Sun analyzed the data, interpreted the data and reviewed the draft of the manuscript. All authors have read and approved the manuscript.

Competing interests

The authors state that there are no conflicts of interest to disclose.

References

1. Zhao J, Frøkjaer JB, Drewes AM, et al. Upper gastrointestinal sensory-motor dysfunction in diabetes mellitus. World J Gastroenterol. 2006; 12(18): 2846–2857, doi: 10.3748/wjg.v12.i18.2846, indexed in Pubmed: 16718808.
2. Ramzan Z, Duffy F, Gomez J, et al. Continuous glucose monitoring in gastroparesis. Dig Dis Sci. 2011; 56(9): 2646–2655, doi: 10.1007/s10620-011-1810-z, indexed in Pubmed: 21735078.
3. Hrdinka M, Yabal M. Inhibitor of apoptosis proteins in human health and disease. Genes Immun. 2019; 20(8): 641–650, doi: 10.1038/s41435-019-0078-8, indexed in Pubmed: 31110240.
4. Zhang MH, Fang XS, Guo JY, et al. Effects of AMPK on apoptosis and energy metabolism of gastric smooth muscle cells in rats with diabetic gastroparesis. Cell Biochem Biophys. 2019; 77(2): 165–177, doi: 10.1007/s12013-019-00870-9, indexed in Pubmed: 30968342.
5. Pang L, Yang K, Zhang Z. High-glucose environment accelerates annulus fibrosus cell apoptosis by regulating endoplasmic reticulum stress. Biosci Rep. 2020; 40(7), doi: 10.1042/BSR20200262, indexed in Pubmed: 32515472.
6. Yang M, Lin Y, Wang Y, et al. High-glucose induces cardiac myocytes apoptosis through Foxo1/GRK2 signaling pathway. Biochem Biophys Res Commun. 2019; 513(1): 154–158, doi: 10.1016/j.bbrc.2019.03.193, indexed in Pubmed: 30952428.
7. Meng S, Cao J, He Q, et al. Metformin activates AMP-activated protein kinase by promoting formation of the $\alpha\beta\gamma$ heterotrimeric complex. J Biol Chem. 2015; 290(6): 3793–3802, doi: 10.1074/jbc.M114.604421, indexed in Pubmed: 25538235.
8. Nambam B, Schatz D. Growth hormone and insulin-like growth factor-I axis in type 1 diabetes. Growth Horm IGF Res. 2018; 38: 49–52, doi: 10.1016/j.ghir.2017.12.005, indexed in Pubmed: 29249623.
9. Li H, Kong R, Wan B, et al. Initiation of PI3K/AKT pathway by IGF-1 decreases spinal cord injury-induced endothelial apoptosis and microvascular damage. Life Sci. 2020; 263: 118572, doi: 10.1016/j.lfs.2020.118572, indexed in Pubmed: 33065147.
10. Luo Li, Lu AM, Wang Y, et al. Chronic resistance training activates autophagy and reduces apoptosis of muscle cells by modulating IGF-1 and its receptors, Akt/mTOR and Akt/FOXO3a signaling in aged rats. Exp Gerontol. 2013; 48(4): 427–436, doi: 10.1016/j.exger.2013.02.009, indexed in Pubmed: 23419688.
11. Vanamala J, Reddivari L, Radhakrishnan S, et al. Resveratrol suppresses IGF-1 induced human colon cancer cell proliferation and elevates apoptosis via suppression of IGF-1R/Wnt and activation of p53 signaling pathways. BMC Cancer. 2010; 10: 238, doi: 10.1186/1471-2407-10-238, indexed in Pubmed: 20504360.

12. Zhang MH, Jiang JZ, Cai YL, et al. Significance of dynamic changes in gastric smooth muscle cell apoptosis, PI3K-AKT-mTOR and AMPK-mTOR signaling in a rat model of diabetic gastroparesis. Mol Med Rep. 2017; 16(2): 1530–1536, doi: 10.3892/mmr.2017.6764, indexed in Pubmed: 28627597.
13. Fang XS, Zhang MH, Zhang XZ, et al. Insulin-like growth factor-1 inhibits the apoptosis of rat gastric smooth muscle cells cultured under high glucose condition through PI3K-Akt-PKC-Ca2+ pathway. Biotechnology & Biotechnological Equipment. 2019; 33(1): 456–464, doi: 10.1080/13102818.2019.1585206.
14. Miricescu D, Totan A, Stanescu-Spinu II, et al. PI3K/AKT/mTOR signaling pathway in breast cancer: from molecular landscape to clinical aspects. Int J Mol Sci. 2020; 22(1), doi: 10.3390/ijms22010173, indexed in Pubmed: 33375317.
15. Martini M, De Santis MC, Braccini L, et al. PI3K/AKT signaling pathway and cancer: an updated review. Ann Med. 2014; 46(6): 372–383, doi: 10.3109/07853890.2014.912836, indexed in Pubmed: 24897931.
16. Yan J, Wang C, Jin Y, et al. Catalpol ameliorates hepatic insulin resistance in type 2 diabetes through acting on AMPK/NOX4/PI3K/AKT pathway. Pharmacol Res. 2018; 130: 466–480, doi: 10.1016/j.phrs.2017.12.026, indexed in Pubmed: 29284152.
17. Liu Y, Deng J, Fan D. Ginsenoside Rk3 ameliorates high-fat-diet/streptozocin induced type 2 diabetes mellitus in mice via the AMPK/Akt signaling pathway. Food Funct. 2019; 10(5): 2538–2551, doi: 10.1039/c9fo00095j, indexed in Pubmed: 30993294.
18. Ersahin T, Tuncbag N, Cetin-Atalay R. The PI3K/AKT/mTOR interactive pathway. Mol Biosyst. 2015; 11(7): 1946–1954, doi: 10.1039/c5mb00101c, indexed in Pubmed: 25924008.
19. Shariati M, Meric-Bernstam F. Targeting AKT for cancer therapy. Expert Opin Investig Drugs. 2019; 28(11): 977–988, doi: 10.1080/13543784.2019.1676726, indexed in Pubmed: 31594388.
20. Yin H, Zhao L, Li S, et al. Impaired cellular energy metabolism contributes to duck-enteritis-virus-induced autophagy via the AMPK-TSC2-MTOR signaling pathway. Front Cell Infect Microbiol. 2017; 7: 423, doi: 10.3389/fcimb.2017.00423, indexed in Pubmed: 29018776.
21. McCampbell AS, Mittelstadt ML, Dere R, et al. Loss of p27 associated with risk for endometrial carcinoma arising in the setting of obesity. Curr Mol Med. 2016; 16(3): 252–265, doi: 10.2174/1566524016666160225153307, indexed in Pubmed: 26917264.
22. Bonucci M, Kuperwasser N, Barbe S, et al. mTOR and S6K1 drive polycystic kidney by the control of Afadin-dependent oriented cell division. Nat Commun. 2020; 11(1): 3200, doi: 10.1038/s41467-020-16978-z, indexed in Pubmed: 32581239.
23. Rozas NS, Redell JB, Hill JL, et al. Genetic activation of mTORC1 signaling worsens neurocognitive outcome after traumatic brain injury. J Neurotrauma. 2015; 32(2): 149–158, doi: 10.1089/neu.2014.3469, indexed in Pubmed: 25025304.
24. Al-Attar R, Childers CL, Nguyen VuC, et al. Differential protein phosphorylation is responsible for hypoxia-induced regulation of the Akt/mTOR pathway in naked mole rats. Comp Biochem Physiol A Mol Integr Physiol. 2020; 242: 110653, doi: 10.1016/j.cbpa.2020.110653, indexed in Pubmed: 31926299.
25. Al Dera H, Eleawa SM, Al-Hashem FH, et al. Enhanced hepatic insulin signaling in the livers of high altitude native rats under basal conditions and in the livers of low altitude native rats under insulin stimulation: a mechanistic study. Arch Physiol Biochem. 2017; 123(3): 145–158, doi: 10.1080/13813455.2016.1275701, indexed in Pubmed: 28084108.
26. Saxton RA, Sabatini DM. mTOR signaling in growth, metabolism, and disease. Cell. 2017; 168(6): 960–976, doi: 10.1016/j.cell.2017.02.004, indexed in Pubmed: 28283069.
27. Sangaunchom P, Dharmasaroja P. Caffeine potentiates ethanol-induced neurotoxicity through mTOR/p70S6K/4E-BP1 Inhibition in SH-SY5Y Cells. Int J Toxicol. 2020; 39(2): 131–140, doi: 10.1177/1091581819900150, indexed in Pubmed: 31955628.
28. Mukaida S, Evans BA, Bengtsson T, et al. Adrenoceptors promote glucose uptake into adipocytes and muscle by an insulin-independent signaling pathway involving mechanistic target of rapamycin complex 2. Pharmacol Res. 2017; 116: 87–92, doi: 10.1016/j.phrs.2016.12.022, indexed in Pubmed: 28025104.
29. Sutton LP, Caron MG. Essential role of D1R in the regulation of mTOR complex1 signaling induced by cocaine. Neuropharmacology. 2015; 99: 610–619, doi: 10.1016/j.neuropharm.2015.08.024, indexed in Pubmed: 26314207.
30. Zhang XH, Chen SY, Tang L, et al. Myricetin induces apoptosis in HepG2 cells through Akt/p70S6K/bad signaling and mitochondrial apoptotic pathway. Anticancer Agents Med Chem. 2013; 13(10): 1575–1581, doi: 10.2174/18715206136661311250123059, indexed in Pubmed: 23438827.
31. Ragan TJ, Ross DB, Keshwani MM, et al. Expression, purification, and characterization of a structurally disordered and functional C-terminal autoinhibitory domain (AID) of the 70 kDa 40S ribosomal protein S6 kinase-1 (S6K1). Protein Expr Purif. 2008; 57(2): 271–279, doi: 10.1016/j.pep.2007.09.014, indexed in Pubmed: 17980619.
32. Keshwani MM, von Daake S, Newton AC, et al. Hydrophobic motif phosphorylation is not required for activation loop phosphorylation of p70 ribosomal protein S6 kinase 1 (S6K1). J Biol Chem. 2011; 286(26): 23552–23558, doi: 10.1074/jbc.M111.258004, indexed in Pubmed: 21561857.
33. Magnuson B, Ekim B, Fingar DC. Regulation and function of ribosomal protein S6 kinase (S6K) within mTOR signalling networks. Biochem J. 2012; 441(1): 1–21, doi: 10.1042/BJ20110892, indexed in Pubmed: 22168436.
34. Cheng CY, Kao ST, Lee YC. Ferulic acid ameliorates cerebral infarction by activating Akt/mTOR/4E-BP1/Bcl-2 anti-apoptotic signaling in the penumbral cortex following permanent cerebral ischemia in rats. Mol Med Rep. 2019; 19(2): 792–804, doi: 10.3892/mmr.2018.9737, indexed in Pubmed: 30569126.
35. Cheng CY, Kao ST, Lee YC. Ferulic acid ameliorates cerebral infarction by activating Akt/mTOR/4E-BP1/Bcl-2 anti-apoptotic signaling in the penumbral cortex following permanent cerebral ischemia in rats. Mol Med Rep. 2019; 19(2): 792–804, doi: 10.3892/mmr.2018.9737, indexed in Pubmed: 30569126.
36. Qin X, Jiang B, Zhang Y. 4E-BP1, a multifactor regulated multifunctional protein. Cell Cycle. 2016; 15(6): 781–786, doi: 10.1080/15384101.2016.1151581, indexed in Pubmed: 26901143.
37. So L, Lee J, Palafox M, et al. The 4E-BP-eIF4E axis promotes rapamycin-sensitive growth and proliferation in lymphocytes. Sci Signal. 2016; 9(430): ra57, doi: 10.1126/scisignal.aad8463, indexed in Pubmed: 27245614.
38. Lieschke E, Wang Z, Kelly GL, et al. Discussion of some 'knowns' and some 'unknowns' about the tumour suppressor p53. J Mol Cell Biol. 2019; 11(3): 212–223, doi: 10.1093/jmcb/mjy077, indexed in Pubmed: 30496435.
39. Liu Y, Tavana O, Gu W. p53 modifications: exquisite decorations of the powerful guardian. J Mol Cell Biol. 2019; 11(7): 564–577, doi: 10.1093/jmcb/mjz060, indexed in Pubmed: 31282934.

40. Karimian A, Ahmadi Y, Yousefi B. Multiple functions of p21 in cell cycle, apoptosis and transcriptional regulation after DNA damage. DNA Repair (Amst). 2016; 42: 63–71, doi: 10.1016/j.dnarep.2016.04.008, indexed in Pubmed: 27156098.
41. Yu D, Liu Q, Qiao Bo, et al. Exposure to acrylamide inhibits uterine decidualization via suppression of cyclin D3/p21 and apoptosis in mice. J Hazard Mater. 2020; 388: 121785, doi: 10.1016/j.jhazmat.2019.121785, indexed in Pubmed: 31818667.
42. Kaluzki I, Hailemariam-Jahn T, Doll M, et al. Dimethylfumarate inhibits colorectal carcinoma cell proliferation: evidence for cell cycle arrest, apoptosis and autophagy. Cells. 2019; 8(11), doi: 10.3390/cells8111329, indexed in Pubmed: 31661890.
43. He P, Li Z, Xu F, et al. AMPK activity contributes to G2 Arrest and DNA damage decrease via p53/p21 pathways in oxidatively damaged mouse zygotes. Front Cell Dev Biol. 2020; 8: 539485, doi: 10.3389/fcell.2020.539485, indexed in Pubmed: 33015052.
44. Yang D, Zhang Qi, Ma Y, et al. Augmenting the therapeutic efficacy of adenosine against pancreatic cancer by switching the Akt/p21-dependent senescence to apoptosis. EBioMedicine. 2019; 47: 114–127, doi: 10.1016/j.ebiom.2019.08.068, indexed in Pubmed: 31495718.
45. McConkey D, Orrenius S. The role of calcium in the regulation of apoptosis. Biochem Biophys Res Commun. 1997; 239(2): 357–366, doi: 10.1006/bbrc.1997.7409, indexed in Pubmed: 9344835.
46. Finkelstein M, Etkovitz N, Breitbart H. Ca signaling in mammalian spermatozoa. Mol Cell Endocrinol. 2020; 516: 110953, doi: 10.1016/j.mce.2020.110953, indexed in Pubmed: 32712383.
47. Makhlouf G, Murthy K. Signal transduction in gastrointestinal smooth muscle. Cell Signal. 1997; 9(3-4): 269–276, doi: 10.1016/s0898-6568(96)00180-5.
48. Nalli AD, Kumar DP, Al-Shboul O, et al. Regulation of G$\beta\gamma$i-dependent PLC-β3 activity in smooth muscle: inhibitory phosphorylation of PLC-β3 by PKA and PKG and stimulatory phosphorylation of Gαi-GTPase-activating protein RGS2 by PKG. Cell Biochem Biophys. 2014; 70(2): 867–880, doi: 10.1007/s12013-014-9992-6, indexed in Pubmed: 24777815.
49. Simon B, Huart AS, Temmerman K, et al. Molecular mechanisms of protein kinase regulation by calcium/calmodulin. Bioorg Med Chem. 2015; 23(12): 2749–2760, doi: 10.1016/j.bmc.2015.04.051, indexed in Pubmed: 25963826.
50. Banerjee C, Khatri P, Raman R, et al. Role of calmodulin-calmodulin kinase II, cAMP/protein kinase A and ERK 1/2 on Aeromonas hydrophila-induced apoptosis of head kidney macrophages. PLoS Pathog. 2014; 10(4): e1004018, doi: 10.1371/journal.ppat.1004018, indexed in Pubmed: 24763432.
51. Jayanthi LD, Wilson JJ, Montalvo J, et al. Differential regulation of mammalian brain-specific proline transporter by calcium and calcium-dependent protein kinases. Br J Pharmacol. 2000; 129(3): 465–470, doi: 10.1038/sj.bjp.0703071, indexed in Pubmed: 10711344.

Submitted: 17 July, 2021
Accepted after reviews: 27 January, 2022
Available as AoP: 14 February, 2022